

# **Thermally Robust Optical Semiconductor Devices Using Molecular Beam Epitaxy Grown AlGaInAs**

Sol P. DiJaili  
Jeffrey D. Walker

December 1997



Lawrence  
Livermore  
National  
Laboratory

This is an informal report intended primarily for internal or limited external distribution. The opinions and conclusions stated are those of the author and may or may not be those of the Laboratory.

Work performed under the auspices of the U.S. Department of Energy by the Lawrence Livermore National Laboratory under Contract W-7405-ENG-48.

# DISCLAIMER

This document was prepared as an account of work sponsored by an agency of the United States Government. Neither the United States Government nor the University of California nor any of their employees, makes any warranty, express or implied, or assumes any legal liability or responsibility for the accuracy, completeness, or usefulness of any information, apparatus, product, or process disclosed, or represents that its use would not infringe privately owned rights. Reference herein to any specific commercial product, process, or service by trade name, trademark, manufacturer, or otherwise, does not necessarily constitute or imply its endorsement, recommendation, or favoring by the United States Government or the University of California. The views and opinions of authors expressed herein do not necessarily state or reflect those of the United States Government or the University of California, and shall not be used for advertising or product endorsement purposes.

This report has been reproduced  
directly from the best available copy.

Available to DOE and DOE contractors from the  
Office of Scientific and Technical Information  
P.O. Box 62, Oak Ridge, TN 37831  
Prices available from (615) 576-8401, FTS 626-8401

Available to the public from the  
National Technical Information Service  
U.S. Department of Commerce  
5285 Port Royal Rd.,  
Springfield, VA 22161

# **Thermally Robust Optical Semiconductor Devices using Molecular Beam Epitaxy grown AlGaInAs**

**Sol P. DiJaili and Jeffrey D. Walker**

## **Abstract**

In FY96, we proposed and demonstrated a thermally robust semiconductor optical amplifier at 1.5  $\mu\text{m}$  wavelength. The novel contributions were the use of a thermally robust gain medium at 1.5  $\mu\text{m}$  wavelength and the use of a highly thermally conductive dielectric used in the fabrication of the SOA. The devices possessed high gain, over 30 dB, and thermally robust behavior in pulsed operation from 60 to 80 degrees C.

In FY97, we proposed and demonstrated the necessary components in a thermally robust long wavelength vertical cavity surface emitting laser (VCSEL) diode. A highly thermally conductive and high reflectivity mirror process was developed for the 1.3  $\mu\text{m}$  or 1.5  $\mu\text{m}$  wavelength region. The thermal conductivity is several times larger than other published work and the reflectivity is greater than 99% . Thermally robust gain media, AlGaInAs/InP quantum wells, were developed at 1.3 and 1.5  $\mu\text{m}$  wavelengths for incorporation into the thermally robust, long wavelength VCSEL devices. Also, a unique and compact high-speed fiber optics package was developed for long wavelength semiconductor optical amplifiers (SOA) and laser diodes.

## **Introduction**

In this proposal, we are addressing the problem of the thermal sensitivity of optoelectronic devices at 1.3 and 1.5  $\mu\text{m}$  wavelength operation. The reasons for the thermal sensitivity are that the usual semiconductor material used for the active gain region, InGaAsP, suffers poor electron confinement and Auger recombination, a strongly temperature dependent nonradiative recombination mechanism. The poor electron confinement is due to small conduction band offsets of the active region with respect to the surrounding cladding. Our solution is twofold. First, we employ a thermally robust gain material AlGaInAs/InGaAs that has shown excellent thermal characteristics for laser diodes at 1.3 and 1.5  $\mu\text{m}$  wavelengths. Second, we employ a highly thermally conductive dielectric material near the

active region that both provides optical confinement and conduct heat away from the active region where most of the heat is generated.

The 1.3 and 1.5  $\mu\text{m}$  optical semiconductor devices that are most sensitive to thermal management are semiconductor optical amplifiers (SOAs) and vertical-cavity surface-emitting lasers (VCSELs). SOAs are sensitive to thermal management because the carrier density level in an SOA is typically a factor of three higher than in a good laser diode design. Thus, Auger recombination is almost a factor of 30 higher since it depends on the cube of the carrier density. VCSELs are sensitive to thermal management both because they share the higher carrier density of SOAs, and because the thermal conductivity between the active region of a VCSEL and the heat-sink is poor. VCSELs require high carrier densities because the gain region length is only a few hundred Angstroms long as compared to a few hundred microns for a typical edge-emitting device, and thus VCSELs require a high gain per unit length. The thermal heat sinking is low in VCSELs because the heat sensitive active region is separated from the heat sink by a 99.5% dielectric mirror. In existing work, this mirror is either a GaAs/AlAs quarter-wave stack and has poor thermal conductance because it is 5  $\mu\text{m}$  thick due to the small available refractive index step, or it is a SiO<sub>2</sub>/TiO<sub>2</sub> type quarter-wave stack and has poor thermal conductance because the thermal conductivity of conventional dielectric materials such as SiO<sub>2</sub> is an order of magnitude lower than that of semiconductors. Ultimately, we hope employ the use two-fold approach of thermally robust gain material and high thermal conductivity dielectrics to improve the performance and lifetime of these long-wavelength optical devices. Another goal of this project is to help support LLNL programs such as ASCI and NAI.

Briefly, we will describe a semiconductor optical amplifier. The basic function of any optical amplifier is to make the light intensity brighter. In the case of a high performance SOA, the light is made brighter by about one thousand times or 30 dB. This number is reduced by input and output fiber coupling losses which can be around 6 dB total. Figure 1 shows a schematic of a ridge waveguide SOA. The light is confined in two dimensions by an optical waveguide. The p-type and n-type semiconductor regions have a lower index than the intrinsic region thus forming an optical waveguide in the vertical direction. In the

horizontal direction, a waveguide is formed by the etching of the ridge. Outside the ridge, the effective index for the optical mode is lower than in the center since the index for the dielectric is made lower than the p-type semiconductor. The ridge height is critically adjusted to keep the waveguide single mode in the horizontal direction. The ridge width is typically about 5  $\mu\text{m}$ . The light beam propagates down the ridge waveguide. The length of the device is approximately 1000  $\mu\text{m}$ . Gain is provided by the process of stimulated emission that occurs in the intrinsic or active region. By injecting current through the device, holes are injected into the intrinsic region from the p-type region and electrons, at a higher energy, are injected in from the n-type region. The electrons and holes recombine and give off the energy in the form of light. If a light beam is present, then the release of energy will be “stimulated” and the net effect is a coherent addition of energy to the original light beam. Thus, as the beam propagates down the ridge waveguide it gets brighter and brighter. Ultimately, saturation of the gain due to the signal and spontaneous emission sets an upper limit on the amount of gain that can be obtained.

Optical amplifiers are used to make up for losses in the transmission of an optical signal. The losses can arise from serial transmission of a light beam in an optical fiber. The amplifier is used in a fiber optic link as a booster, regenerator, or preamplifier between the transmitter and receiver. Also, as optical networks become more prevalent, losses can occur from the distribution of the signal to many users or by splitting losses in a switched network. Optical amplifiers can be used to make up for splitting losses as well. For semiconductor optical amplifiers, the advantages over other types of optical amplifiers are in cost, size, and the fact that they can be switched over six orders of magnitude faster than the doped fiber amplifiers. The main problem preventing their widespread use has been the problem of crosstalk between different wavelength channels and gain recovery in the time domain. These problems arise from the dynamic gain variations that occur in the SOA. Recently, we have demonstrated a solution to this problem that we believe will enable the widespread deployment of SOAs [1].

Because we support the LLNL programs, when 1.5 $\mu\text{m}$  SOA chips became commercially attainable earlier this year, we shifted our 1.5 $\mu\text{m}$  conventional SOA effort to packaging of

commercially available chips, and focused the current work on long-wavelength VCSELs. Long-wavelength VCSELs are an extremely challenging problem that will pay off in the development of both parallel optical interconnects with significant improvements in bandwidth-distance product over existing shorter wavelength technology [2]. Also, long wavelength crosstalk-free SOAs, that are very dependent on long wavelength VCSELs, will allow greatly decreased size/weight/cost and increased functionality of fiberoptic systems. An example of an important programmatic application of crosstalk-free SOAs is in lightweight remote sensing systems. Both of these applications are excellent examples of dual-use technology. This report reviews our progress on unique packaging of 1.5  $\mu\text{m}$  SOAs, and on thermally robust gain regions and dielectric mirrors for applications to long wavelength VCSELs.

A VCSEL differs from a conventional laser diode in that it emits light vertically out of the top surface of the chip, rather than out of the cleaved edge. VCSELs have shown much promise for applications such as parallel optical interconnects and other low-cost optoelectronics applications, however, they pose technical problems that are extremely challenging to solve as compared to edge-emitting laser diodes, and they are just now becoming commercially available for very limited applications. The fundamental challenge stems from the fact that in a VCSEL, the gain region length is limited to a few hundred angstroms rather than a few hundred microns of a edge-emitting “waveguide” device. As a result, the available round-trip optical gain in a VCSEL is on the order of 1% rather than a hundred thousand percent. This in turn requires that the total round-trip mirror loss be on the order of 1%, e.g. both mirrors are 99.5% reflective. Because metals such as silver only have reflectivities on the order of 90%, dielectric mirrors made of quarter-wavelength thick layers of either semiconductors such as GaAs/AlAs or conventional dielectrics such as SiO<sub>2</sub>/TiO<sub>2</sub> are used to get the high reflectivities required. These tight requirements on round-trip gain and loss have made the development of vertical-cavity lasers an extremely challenging task. The first robust 0.8/1.0  $\mu\text{m}$  VCSELs were first demonstrated in 1990, and robust 1.3/1.5  $\mu\text{m}$  VCSELs have not yet been demonstrated, although the scientific community is getting very close to demonstrating robust long wavelength devices [3,4]. One of the key problems with existing long-wavelength VCSEL demonstrations is the thermal management issue that is addressed in this project.

## RESULTS:

### A) Demonstration of 1.5 $\mu\text{m}$ semiconductor optical amplifiers:

Figure 2 shows the band diagram for the active regions and surrounding p and n type material. The carriers (electrons and holes) are confined to the active region by the increase in the band gap energies between the active region and the surrounding n and p-type regions. As the temperature is increased, the resulting electron energy distribution causes the higher energy electrons to surmount the band gap of the n or p type regions and leak out of the active region. The effective mass of the electrons is much lighter than that of the holes and the loss of carriers due to thermionic emission out of the active regions tends to be dominated by the electrons. The quantum wells provide improved carrier confinement and make the stimulated emission of photons more efficient. In the case of the AlGaInAs/InGaAs, the difference in energies in the conduction band between the bottom of the quantum well and the conduction band in the n or p-type regions is around 500 meV. This energy difference compares quite favorably to the energy differences in the conventional material used at 1.5  $\mu\text{m}$  wavelength. For InGaAsP active regions and InP n and p type regions, the energy difference is around 300 meV. Also, in the case of the AlGaInAs/InGaAs material system, strained InGaAs quantum wells are used. In an energy versus momentum diagram, this strain causes the light and heavy hole bands to split in energy. The result is that conservation of energy and momentum required for Auger recombination to occur is significantly reduced. Auger recombination is a non radiative recombination mechanism between the electrons in the conduction band and holes in the valence band and thus suppresses efficient stimulated emission.

The molecular beam epitaxy (MBE) machine was used to grow the thermally robust material. In order to grow high quality AlGaInAs films on InP substrates, high quality epitaxial InP needs to be grown. To accomplish this, a solid source phosphide cracker was prepared and installed into the MBE. The film stacks that were grown consisted of a n-type InP buffer, a n-type AlGaInAs region, a graded AlGaInAs region to a lower energy band gap, an intrinsic region consisting of AlGaInAs barriers and InGaAs quantum wells, a graded AlGaInAs region to a higher energy band gap, a p-type AlGaInAs region, a p-

type InP buffer region, and a p-type InGaAs cap layer. All the layers were lattice matched to the lattice constant of InP except for the InGaAs where an approximate 0.7 percent tensile strain was introduced. An x-ray diffractometer was set-up and the lattice match conditions were measured. Several wafers were grown and the MBE growth conditions were adjusted to achieve the necessary lattice match conditions. Broad area lasers were processed from the resulting laser material and the laser thresholds were measured. A laser threshold current density of  $400 \text{ A/cm}^2$  was achieved. For MBE grown AlGaInAs/InGaAs, this performance number is the best by a significant margin as compared to currently published work.

The laser wafer material was then processed into ridge waveguides using a self-aligned process developed at LLNL. The ridges were tilted at 7 degrees with respect to the (011) crystal plane. The etch process was developed so that smooth and controlled etches are achieved on InP. A self-aligned and highly thermally conductive dielectric was deposited using a magnetron sputtering machine. The device is self-aligned since the electrical contact opening in the dielectric and the top of the ridge waveguide are intrinsically aligned in the process. This dielectric provides a lower index of refraction so that a waveguide is achieved in the lateral direction. Also, it provides for a highly thermally conductive material that has a significantly higher thermal conductivity than regrown InP. The devices are cleaved along the crystal planes. The tilt in the ridge with respect to the crystal facet is used to suppress the coupling of the back reflection into the guided mode. The back reflections into the guided mode should be reduced to about  $10^{-4}$  otherwise undue spectral gain ripple or lasing can occur. The process is routinely performed and good yields are achieved.

A plot of the amplified spontaneous emission (ASE) versus wavelength from the device is shown in figure 3. The output was taken with a multi-mode fiber coupled to the output of the SOA. The signal was measured using an optical spectrum analyzer with a 10 nm resolution bandwidth. The center wavelength is at 1535 nm and the full width at half maximum (FWHM) is approximately 60 nm. The operating current for the device was 300 mA. The FWHM of 60 nm represents about 8 THz of optical bandwidth.

To facilitate rapid measurements of the gain of the device, we used a power meter to measure the ASE power output of the device. The formula for ASE power coupled into the guided mode of the SOA is given by  $P_{\text{ASE}} = 2 h\nu \Delta\nu (G - 1) \chi$ .  $G$  is the gain of the SOA. The parameter  $h\nu$  is the photon energy at 1.5  $\mu\text{m}$  wavelength. The parameter  $\Delta\nu$  represents the optical bandwidth of the ASE spectra and  $\chi$  represents the amount of inversion in the gain medium and ranges from 1 to 3 dB in value. Thus, by measuring the ASE power output, we can obtain a rapid measurement of the gain present. Figure 4a and 4b show the pulsed and CW gain of the SOA device as a function of applied current at various heat sink temperatures. The current pulses were 1  $\mu\text{sec}$  in duration at a 1KHz repetition rate. At room temperature, the SOA device showed a maximum gain of over 35 dB pulsed and 28 dB CW. At 60 degrees C, the device showed 32 dB gain pulsed and 17 dB CW. At 80 degrees C the pulsed gain is still over 20 dB. The pulsed data with temperature being varied indicate the performance of the active region alone. The drop in gain due to CW operation indicates how well the heat is being extracted from the gain region. Unfortunately, the current consumption is quite high. We are taking steps to reduce the current by redesigning the optical mode so that a narrower ridge width and adequate ridge height to reduce current leakage is achieved while still maintaining the effectiveness of the antireflection tilted facets. We are confident that we can achieve a low current consumption device and have the CW gain versus current data approach the pulsed data to within several dB. It should be pointed out that in spite of the high current consumption, the devices, as they stand, can operate to 60 degrees C and still have an adequate gain.

#### **B) Packaging of 1.5 $\mu\text{m}$ optical amplifiers:**

Figure 5 shows a package for the 1.5  $\mu\text{m}$  SOAs. One of the unique and important features of this package is the short length of the total fiber connectorized unit. The utility of such a package is in the fact that there are no long lengths of fiber pigtailling to maneuver and the short length allows for easy incorporation into a modelocked laser cavity configuration with high repetition rate. The overall length of the packaged device is just over 2 inches; however, 60% of this length is due to the connectors. Further development should be able to reduce the overall package size. The package also features a high speed electrical modulation port. Using this port, the SOA can then be used to as a high speed

optical modulator. We have modulated SOAs to 1 Gb/s with low bit error rates using the high speed electrical port. The SOA device, a TE cooler, thermistor, and fibers were attached to LLNL's silicon optical microbench technology (a R&D 100 award winner developed by Mike Pocha).

### **C) Development of a highly thermally conductive, long wavelength dielectric Bragg mirror**

In the course of the development of the appropriate mirror for a long wavelength VCSEL, we imposed several important criteria. First, the mirror ideally would consist of highly thermally conductive dielectric materials while maintaining low optical loss. Second, the various mirror materials should possess large index differences so as to reduce the overall thickness of the mirror, which would reduce the overall thermal resistance. Third, the mirrors should have a very high reflectivity. Ideally, this reflectivity should be greater than 99.5 %. We are not the first to pursue a highly thermally conductive dielectric mirror in the development of long wavelength VCSELs. One other research group has used high thermal conductivity materials in the development of their long wavelength VCSELs [5] ; however, we hope to be the first to combine the highly thermally conductive dielectric mirrors with the thermally robust AlGaInAs gain medium.

Figure 6 illustrates the reflection spectrum of our newly developed mirror. The peak reflectivity at 1.3  $\mu\text{m}$  is approximately greater than 99 %. The number of dielectric pairs used in this mirror was 4 layers. The calibration mirror used was a Newport ER.2 mirror. The specified mirror reflectivity at 1.3  $\mu\text{m}$  wavelength is 98 % according to the Newport catalog. The measured reflectivity appears to be high enough to begin fabrication of a high quality thermally robust long wavelength VCSEL. Of course, in the testing of the device, the reflectivity will be improved and optimized (i.e. more mirror pairs will be added as needed) to achieve the necessary performance. The reflection measurement was performed by using a white light source coupled into 50  $\mu\text{m}$  core / 125  $\mu\text{m}$  cladding multi-mode fiber and then coupled into a 3 dB multi-mode directional coupler. One of the output ports was connected to a GRIN lens collimator. The light was retroreflected from the mirror under test and maximized for coupling. The other input port on the 3 dB coupler was connected to the input of a multi-mode Hewlett-Packard Optical Spectrum Analyzer. The test set-up

was calibrated with the Newport ER.2 mirror discussed above. We are cautious about the ultimate accuracy of measurement technique and the true test is the performance of the VCSELs from the mirrors. The mirror results look quite good as a starting point.

The mirrors were fabricated with a newly commissioned ion beam deposition (IBS) dielectric coater shown in figure 7. The materials that were used was amorphous silicon and aluminum nitride. Appropriate process parameters needed to be properly adjusted in order to achieve low optical losses. One of the apparent advantages of ion beam deposition is that the resultant dielectric films have the highest densities and smoothest surface morphology as compared with other deposition techniques. Significant effort on the part of the team was expended to commission the IBS system into service.

#### **D) Development of the thermally robust gain region at 1.3 $\mu\text{m}$ wavelengths using AlGaInAs**

In parallel to the development of high thermal conductivity VCSEL mirrors, we have also addressed the issue of thermally robust gain regions for long wavelength VCSELs. The use of strain reduces non-radiative Auger recombination, and the use of AlGaInAs instead of the standard InGaAsP materials system reduces carrier loss due to thermionic emission out of the active region. As part of the development of VCSELs, we have extended this work on thermally robust gain regions to the 1.3 $\mu\text{m}$  wavelength region, and demonstrated the first 1.3  $\mu\text{m}$  laser diodes epitaxially grown at LLNL.

The laser design and fabrication were similar to that previously discussed above for the 1.5  $\mu\text{m}$  laser diode devices, except for the quantum well active region that was adjusted to achieve the 1.3  $\mu\text{m}$  lasing wavelength. In the device presented here, a strain-compensated two quantum well active region was used with 80 $\text{\AA}$  thick 1% compressive strained Al(.18)Ga(.12)In(.70)GaAs quantum wells, and a 80 $\text{\AA}$  thick 1% tensile strained Al(.27)Ga(.33)In(.40)As barrier. Aluminum was added to the quantum wells to achieve the 1.3  $\mu\text{m}$  desired lasing wavelength while maintaining a relatively wide 80  $\text{\AA}$  quantum well width. The lasing spectrum of a 1.31  $\mu\text{m}$  laser diode is shown in Figure 8. These lasers had relatively high thresholds of 1 kA/cm<sup>2</sup>, however, part of the reason for the high threshold is the use of this novel materials system and through refinement of epitaxial

growth conditions this number should drop to the 400 A/cm<sup>2</sup> number that we achieved previously for the 1.5  $\mu\text{m}$  devices. Following several iterations to refine the growth conditions, this gain material will be combined with the high thermal conductivity mirrors to fabricate long wavelength vertical-cavity lasers.

### Acknowledgments

The authors would like to acknowledge the diligent efforts of Bill Goward, Holly Petersen, and Phil Stephan. This work was performed under the auspices of the U. S. Department of Energy by Lawrence Livermore National Laboratory under contract No. W-7405-Eng-48.

### References

- [1] J.D. Walker, F.G. Patterson, S.P. Djaili, and R.J. Deri, "A gain-clamped crosstalk free vertical cavity lasing semiconductor optical amplifier for WDM applications," Integrated Photonics Research Conf., Boston, Mass., April 29 - May 2, 1996, paper IWD1.
- [2] P. S. Henry, R. A. Linke, and A. H. Gnauck, "Introduction to lightwave systems", Ch 21, p 796 in *Optical Fiber Telecommunications II*, eds. S. E. Miller and I. P. Kaminow, Academic Press, 1988.
- [3] Y. Qian et al. "Low-threshold proton-implanted 1.3 $\mu\text{m}$  vertical-cavity top-surface-emitting lasers with dielectric and wafer-bonded GaAs-AlAs Bragg mirrors", IEEE PTL **9**(7), 866 (1997).
- [4] T. Baba, Y. Togo, K. Suzuki, F. Koyama, and K. Iga, "Continuous wave GaInAsP/InP surface emitting lasers with a thermally conductive MgO/Si Mirror", Jpn. J. Appl. Phys. **33**, 1905 (1994).

Figures and figure captions:

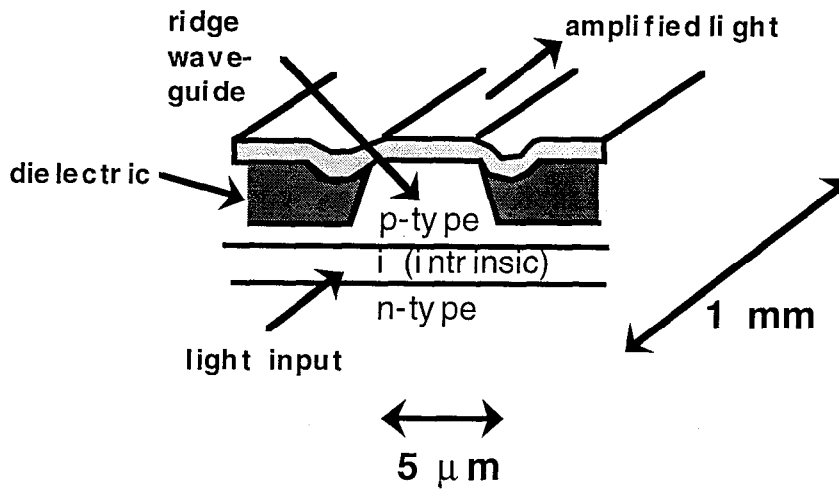


Figure 1. A basic diagram of a semiconductor optical amplifier.

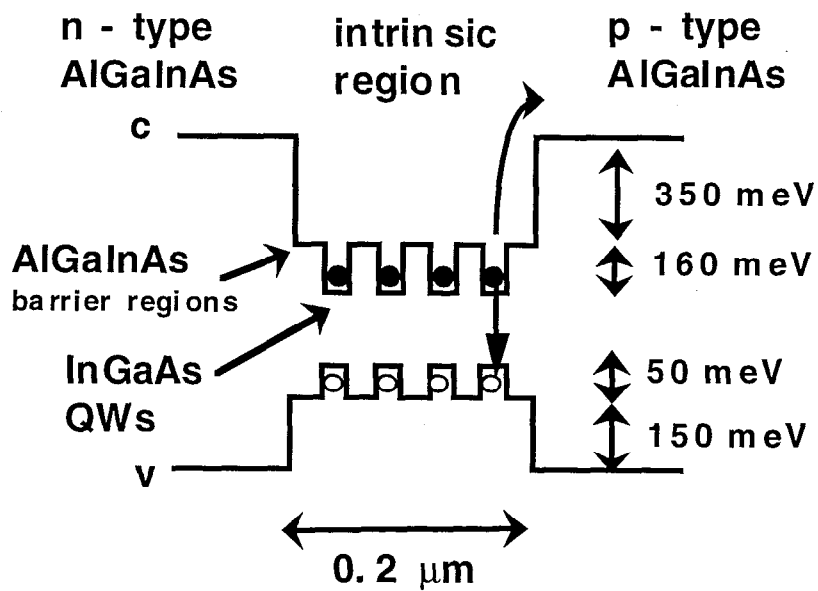


Figure 2. The energy band diagram for the AlGaInAs/InGaAs multi-quantum well heterostructure material.

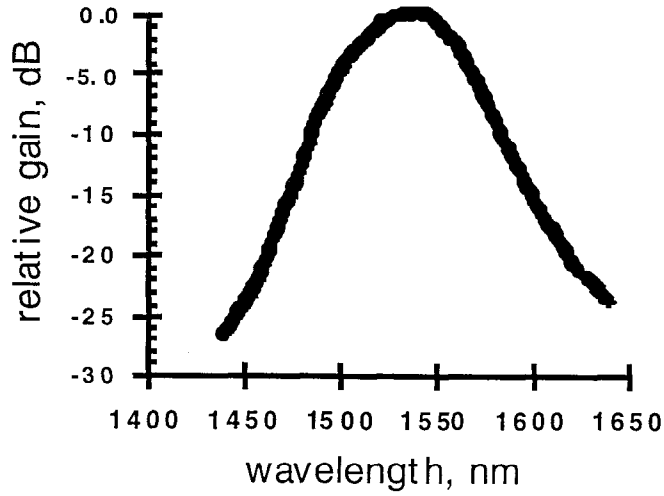


Figure 3. Amplified spontaneous emission spectrum for the 1.5  $\mu\text{m}$  SOA device.

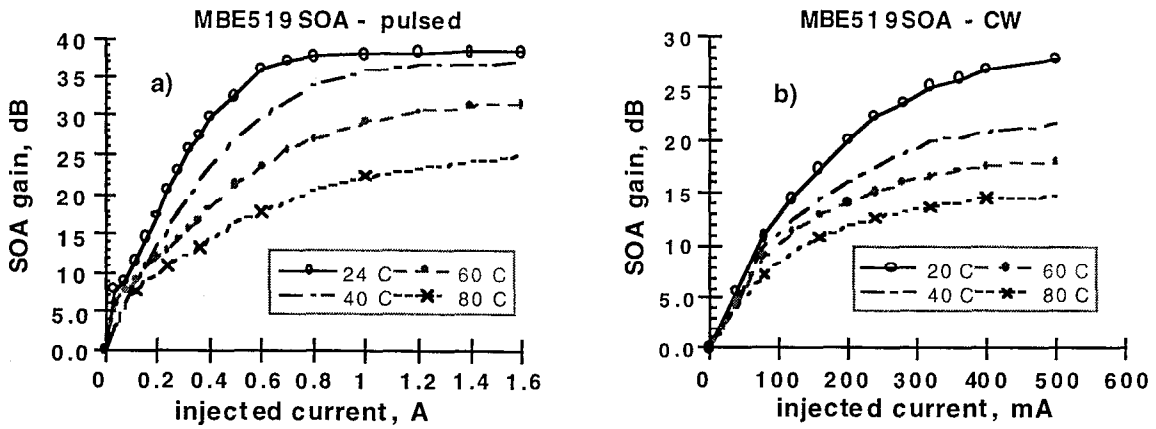


Figure 4 a) and b). Gain versus current at various temperatures for the 1.5  $\mu\text{m}$  SOA.

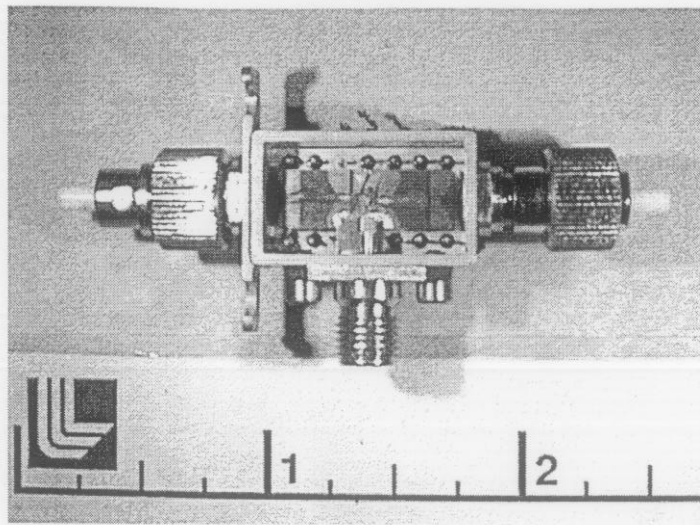


Figure 5. Compact, high-speed SOA package

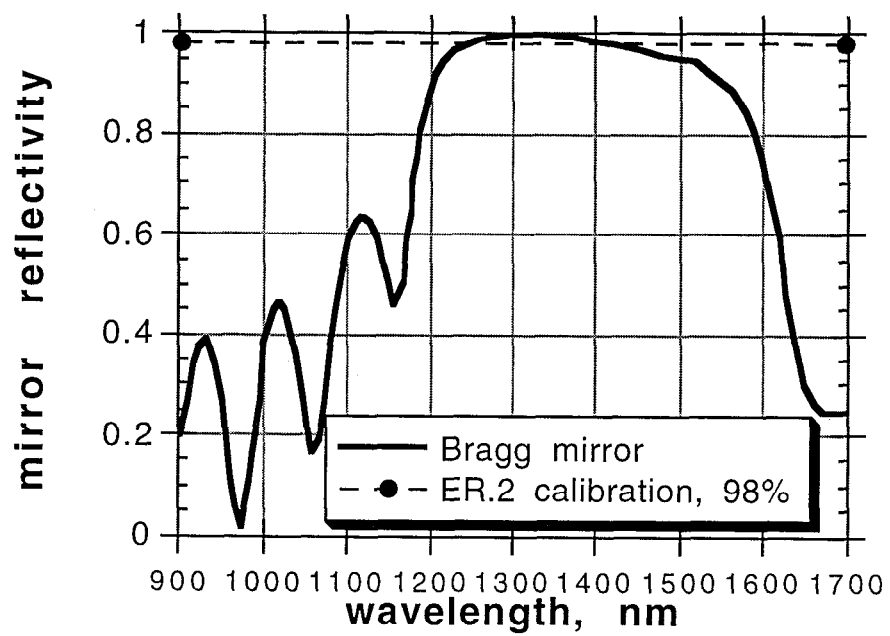


Figure 6. Reflectance spectra of 1.3  $\mu\text{m}$  high thermal conductivity dielectric mirror.

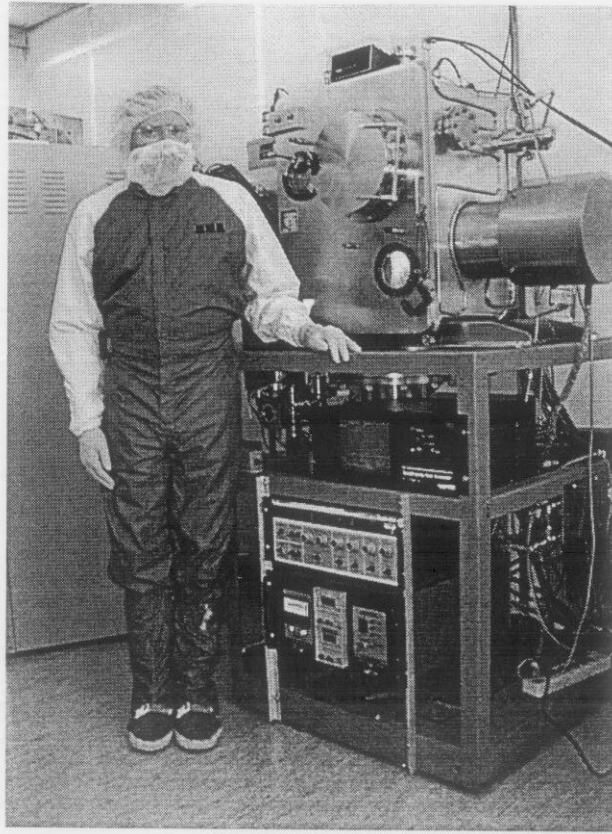


Figure 7. Bill Goward stands in front of the IBS system.